Rapid Communications

Phase-formation diagram for precursors to epitaxial growth of NiSi$_2$ on Si(111)

P. A. Bennett, A. P. Johnson, and B. N. Halawith

Department of Physics, Arizona State University, Tempe, Arizona 85287

(Received 13 August 1987)

Using reflection high-energy electron diffraction and Auger microanalysis in a custom-built ultrahigh vacuum scanning electron microscope we have identified six ordered structures that precede epitaxial NiSi$_2$ during the annealing of nickel overlayers on Si(111). A novel technique of depositing through holes in a mask positioned near the sample allows us to obtain the complete coverage dependence of these structures in a single annealing cycle. The role of these structures in relation to the NiSi$_2$ (B) (twinned) and NiSi$_2$ (A) (nontwinned) structures is described.

Ni/Si(111) is a model system for the study of metal-semiconductor epitaxial growth. The CaF$_2$ crystal structure of NiSi$_2$ has a lattice parameter 0.5% smaller than silicon, resulting in a nearly perfect interface whose structure is known: The nickel atoms are sevenfold coordinated,[1] and even small perturbations of atomic positions at the interface have been determined using ion channeling and blocking techniques.[2] One interesting aspect of this system is the occurrence of "double positioning" of the overlayer, which can be controlled by the deposition conditions in an ultrahigh vacuum (UHV) environment. Thus, a room-temperature deposit of <7 Å nickel followed by annealing to 500 °C results in epitaxial NiSi$_2$ rotated 180° or twinned on the (111) plane (B type), while deposits of 16–20 Å are nontwinned (A type), and thicker coverages are mixed A and B type.[3] This result has been confirmed in numerous other experiments.[4-6] Interest in this system is partly stimulated by the report that the B- and A-type NiSi$_2$ overlayers have significantly different Schottky barrier heights,[7] although this report has been disputed.[4,5]

In an attempt to understand this system, numerous experiments have been done at temperatures below 500 °C seeking precursor structures to the NiSi$_2$ overlayer, yet a clear understanding has not emerged. In thick films and non-UHV conditions, a progression of the stable compounds Ni$_2$Si, NiSi, NiSi$_2$ is observed with increasing annealing temperatures.[8,9] By contrast, the structure of the overlayer formed at room temperature under UHV conditions is not agreed upon. Rutherford backscattering (RBS) experiments show that a chemical reaction takes place already below room temperature.[10] Photoemission experiments find that a graded composition occurs with multiple phases simultaneously present.[11] More recent RBS experiments report that a composition near that of

Ni$_2$Si results for room-temperature coverages below 9 Å.[12] Surface extended x-ray-absorption fine-structure (SEXAFS) studies find that the local environment of nickel is like NiSi$_2$ for a coverage of 1 Å.[13] It is thought in any case that these structures are amorphous, since coverages above a few Å obliterate the low-energy electron diffraction (LEED) pattern.[14] Mild annealing can produce $\sqrt{3}$ or $\sqrt{19}$ superlattices corresponding to unknown structures,[3,15] while a 2×2 superlattice has been reported and identified as NiSi using x-ray photoemission spectroscopy (XPS).[16] In earlier work using reflection high-energy electron diffraction (RHEED) we identified Ni$_2$Si islands and oriented nickel clusters following a mild anneal.[17]

The apparatus for these experiments is a custom-built UHV scanning electron microscope featuring a field emission gun and diffraction capabilities, and is described in detail elsewhere.[17,18] Nickel is deposited from a differentially pumped electron bombardment evaporator whose target is a 12-mm-diameter foil of 99.999% purity. Using an infrared pyrometer, nearly instantaneous readings from a 1-mm-diameter region of the sample are obtained with an accuracy of 5% of the centigrade reading in the range of 250 to 1200 °C. The sample was cleaned *in situ* by several cycles of heating to 1200 °C, after which a sharp 7×7 RHEED pattern with no trace of SiC transmission spots was obtained. The Auger $I(C(KLL))/I(Si(LVV))$ ratio in $E^* dN(E)/dE$ spectra was typically 0.2%. The thickness of nickel deposited was determined by comparing our $I(Ni)/I(Si)$ ratios to those obtained by van Loenen, van der Veen, and LeGoues[12] using similar equipment, and correlating this to their RBS yields. Thus, for room-temperature depositions on Si(111), a $I(Ni/I(Si))$ ratio of 1 corresponds to a coverage of 6×10^{15} cm^2 or 7 Å of amorphous nickel.[19]

Nickel is deposited through 100-μm holes in a mask positioned 300 μm from the sample surface, resulting in graded thickness edges outlining features of the mask. This mask technique follows earlier work by Butz and Wagner[20] and Futamoto et al.[21] Note that the deposition rate in our experiments is exactly proportional to coverage and is typically 0.2 $\mathrm{\AA \, min^{-1} \AA^{-1}}$. The precise form of this concentration profile is easily calculated from the known geometry. We subsequently perform RHEED and Auger microanalysis on a grid of points spanning the concentration profile. The sample is then annealed at a given temperature for 4 min, cooled to room temperature, and the diffraction measurements repeated. We determined that negligible lateral diffusion (on a scale of several microns) occurs during the anneal, since very sharp shadow edges produced by holding the mask closer to the specimen remain unchanged during anneals at temperatures below 700 °C.

Figure 1 (upper panel) shows a dark field image formed using the substrate (400) Kikuchi band, for three such patches of nickel, 40 $\mathrm{\AA}$ thick at their centers after annealing at 600 °C. The four strongly contrasted regions in each patch correspond to Si(111) 7×7, NiSi$_2$ (B), NiSi$_2$ (A), and NiSi$_2$ ($A + B$) in sequence, clearly following the known coverage dependence of these structures. The lower panel is a secondary electron image at lower magnification showing strong, nontopographic contrast from the nickel patches, due to a change in secondary electron yield.[21]

The diffraction patterns from the various phases obtained are shown in Fig. 2, all for the same conditions of 15 keV, 2° glancing angle, and [110] substrate azimuth. Here we present only the results of our analysis of the diffraction patterns, the details appear elsewhere.[22] Panels (A) and (B) correspond to epitaxial NiSi$_2$ A and B type, respectively. They are easily distinguished by the prom-
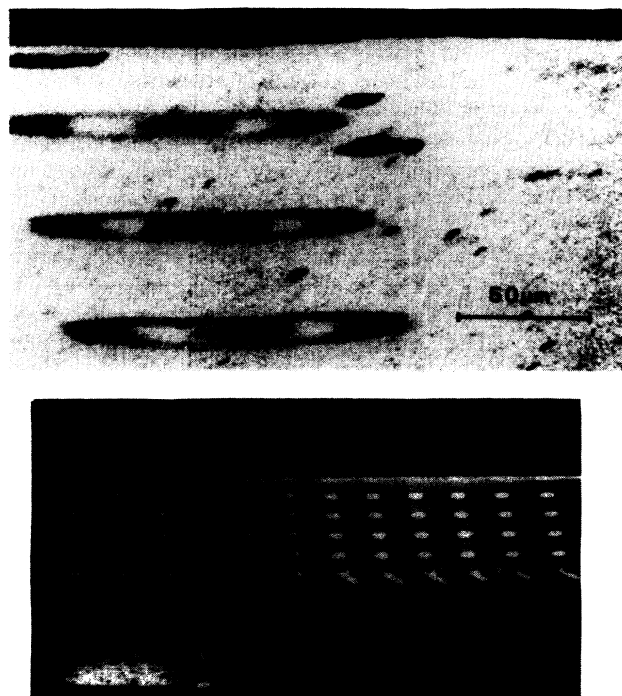

FIG. 1. Dark field image of three annealed patches of nickel showing the NiSi$_2$ (B), NiSi$_2$ (A), and NiSi$_2$ ($A + B$) structures (top panel). Secondary electron image at low magnification (bottom panel).

inent (400) Kikuchi band on the right and left sides of the pattern, respectively. Panel (C) is a transmission pattern from Ni$_2$Si-δ (islands) in the epitaxial relation Ni$_2$Si(010)/Si(111) and Ni$_2$Si(100)/Si(110).[17] This is an orthorhombic structure ($a = 7.06$, $b = 4.99$, $c = 3.72$ $\mathrm{\AA}$) with a nearly hexagonal mesh in the (010) projection
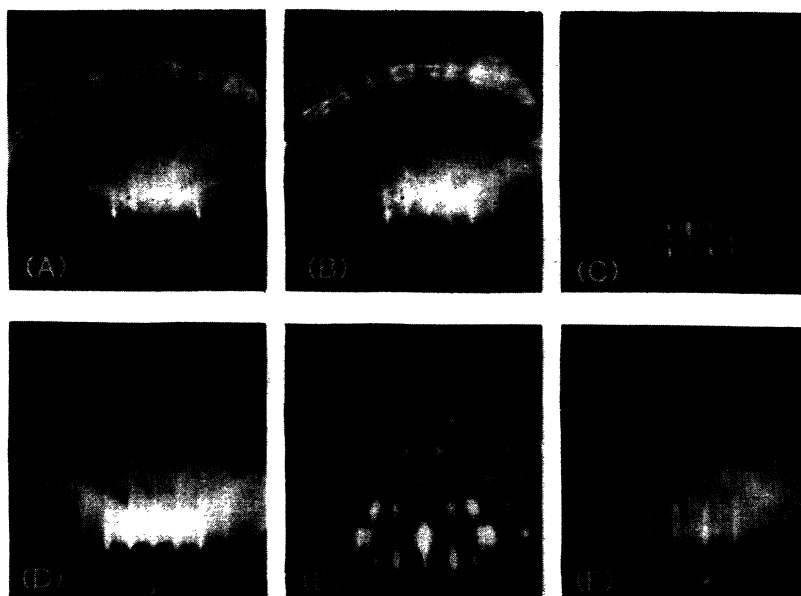

FIG. 2. RHEED patterns at 15 keV, [110] azimuth of (A) NiSi$_2$, (B) NiSi$_2$ (B), (C) Ni$_2$Si-δ (islands), (D) NiSi$_2$ ($A + B$), (E) Ni (islands), and (F) $\alpha + \beta$(NiSi).

whose area is 3% larger than that of the substrate. Panel (D) is a 1×1 RHEED pattern with apparent hexagonal symmetry. We label this as NiSi$_2$ ($A+B$) corresponding to a mixture of NiSi$_2$ (A) and NiSi$_2$ (B). We believe it contains a high density of either twins or stacking faults, which cases we cannot at present distinguish. This phase is identified using the Kikuchi band pattern and RHEED rocking curves, as well as Auger stoichiometry and line-shape analysis.[22] Its presence at low temperatures may be related to the stacking fault nature of the Si(111) 7×7 structure.[23,24] Weak half-order streaks are also visible which we believe correspond to a flat Ni$_2$Si-δ (2×1) structure. That is, the Ni$_2$Si-δ ($1k0$) and ($0k2$) reflections comprise rods with a 2×1 surface mesh. During annealing, the half-order rods disappear quickly leaving a clear 1×1 pattern. Panel (E) is a transmission pattern from nickel (islands) in the epitaxial relation Ni(110)/Si(111) and Ni(100)/Si(110). Panel (F) corresponds to structures we cannot identify from the RHEED patterns alone. The α structure contains large crystallites with a poorly defined habit plane, while the β structure has a lattice spacing of 0.8 times the 1×1 substrate mesh in the [112] direction. Cross-section transmission-electron-microscopy (TEM) samples of a 200-Å overlayer prepared by multiple deposition and anneal cycles under conditions similar to those for this pattern were identified as NiSi (orthorhombic).

The conditions under which the previously described diffraction patterns are observed are shown in the phase formation diagram of Fig. 3. All phases persist after cooling to room temperature. The horizontal axis is thickness of nickel deposited at room temperature and the vertical axis is the temperature of a 4-min anneal. Solid lines denote an abrupt change in the diffraction pattern while dotted lines denote a gradual change, often with a super-position of two or more patterns.

Several features of the phase diagram deserve comment in context of previous work on this system. The thickness transition from NiSi$_2$ (B) to NiSi$_2$ (A) at temperatures above 500 °C agrees with previous results.[4–6] The apparent lack of NiSi$_2$ (B) at coverages below 2 Å is in disagreement with RBS experiments[25] that report island formation of NiSi$_2$ (B) occurring at low coverages, while we see a sudden change in the RHEED pattern as a function of coverage. This is dramatically evident in the dark field image shown in Fig. 1. This may be understood if we assume that the RHEED pattern is only fully developed at the point of island coalescence, illustrating our sensitivity to morphology. The formation of nickel clusters for room-temperature deposits above 12 Å is accompanied by a rapid decrease in the silicon Auger signal, signifying saturation of a mixing reaction that produces the disordered phase at lower coverages. The appearance of ordered Ni$_2$Si-δ (2×1) at $T=250$ °C suggests that the coexisting disordered material is Ni$_2$Si, as described by van Loenen et al.[12] and Fischer et al.[26]
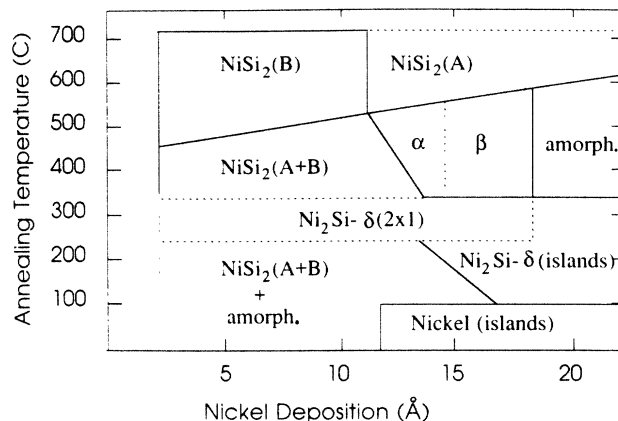

FIG. 3. Phase diagram representation of coverages and annealing temperature conditions under which the silicide structures are observed. Solid lines show distinct boundaries, dotted lines show coexistence.

We observe that the coverage dependence of the precursor structures is strongly correlated with the epitaxial NiSi$_2$ formed at higher temperatures. In particular we note that NiSi$_2$ (B) is preceded in the annealing sequence by Ni$_2$Si ("amorphous" state), Ni$_2$Si-δ (2×1), NiSi$_2$ ($A+B$); while NiSi$_2$ (A) is preceded by Ni (islands), Ni$_2$Si-δ (islands), α (NiSi-misoriented), or β (NiSi-oriented), or "amorphous" state. Thus, the structures preceding NiSi$_2$ (B) are epitaxial with a well-defined habit plane, while those preceding NiSi$_2$ (A) are not. This coverage also marks the transition in the Ni$_2$Si-δ structure from layers to islands. These observations are reminiscent of a well-known phenomenon in epitaxial growth wherein the increasing strain of a lattice mismatched overlayer eventually destroys perfect epitaxy for thickness exceeding a critical value.[27] We note here also that the phase formation diagram is strongly path dependent. For example, deposition at 300 °C (rather than room temperature) followed by annealing results in major qualitative changes.[28] Clearly any model for these structural transitions will have to include explicit kinetic effects.

Note added. Gibson *et al.* have identified an epitaxial Ni$_2$Si-θ phase which preceeds NiSi$_2$ (A) during annealing. We presume that this phase is buried below the α phase in our experiment and does not contribute to the RHEED pattern.

[1]D. Cherns, G. R. Anstis, J. L. Hutchinson, and J. C. H. Spence, Philos. Mag. A **46**, 849 (1982).

[2]E. J. van Loenen, J. W. M. Frenken, J. F. Vander Veen, and S. Valeri, Phys. Rev. Lett. **54**, 827 (1985).

[3]R. T. Tung, J. M. Gibson, and J. M. Poate, Phys. Rev. Lett. **50**, 429 (1983).

[4]M. Liehr, P. E. Schmid, F. K. LeGoues, and P. S. Ho, Phys. Rev. Lett. **54**, 2139 (1985).

[5] R. J. Hauenstein, T. E. Schlesinger, T. C. McGill, B. D. Hunt, and L. J. Schowalter, J. Vac. Sci. Technol. B **4**, 649 (1986).

[6] G. Akinici, T. Ohno, and E. D. Williams, Appl. Phys. Lett. **50**, 754 (1987).

[7] R. T. Tung, Phys. Rev. Lett. **52**, 461 (1984).

[8] K. N. Tu, E. I. Alessandriri, W. K. Chu, H. Krautle, and J. W. Mayer, Jpn. J. Appl. Phys. Suppl. **2**, 669 (1974).

[9] H. Foll, P. S. Ho, and K. N. Tu, Philos. Mag. **45**, 31 (1982).

[10] N. W. Cheung, R. J. Culbertson, L. C. Feldman, P. J. Silverman, K. W. West, and J. W. Mayer, Phys. Rev. Lett. **45**, 120 (1980).

[11] N. W. Cheung, P. J. Grunthaner, F. J. Grunthaner, J. W. Mayer, and B. M. Ullrich, J. Vac. Sci. Technol. **18**, 917 (1981).

[12] E. J. van Loenen, J. F. van der Veen, and F. K. LeGoues, Surf. Sci. **157**, 1 (1985).

[13] F. Comin, J. E. Rowe, and P. H. Citrin, Phys. Rev. Lett. **51**, 2402 (1983).

[14] W. S. Yang, F. Jona, and P. M. Marcus, Phys. Rev. B **28**, 7377 (1983).

[15] J. G. Clabes, Surf. Sci. **145**, 87 (1984).

[16] H. Von Kanel, T. Graf, J. Henz, M. Ospelt, and P. Wachter, J. Cryst. Growth **81**, 470 (1987).

[17] P. A. Bennett, B. N. Halawith, and A. P. Johnson, J. Vac. Sci. Technol. A **5**, 2121 (1987).

[18] B. N. Halawith, M. S. thesis, Arizona State University, 1986 (unpublished).

[19] A smaller value given in Ref. 17 failed to account for a factor E in the EdN/dE spectra of Ref. 12.

[20] R. Butz and H. Wagner, Surf. Sci. **87**, 69 (1979).

[21] M. Futamoto, M. Hanbucken, C. J. Harland, G. W. Jones, and J. A. Venables, Surf. Sci. **150**, 430 (1985).

[22] P. A. Bennett, X. Tong, and J. Butler, in *Proceedings of Physics and Chemistry of Semiconductor Interfaces 15, Asilomar, California, 1988*, [J. Vac. Sci. Technol. (to be published)].

[23] P. A. Bennett, L. C. Feldman, Y. Kuk, E. G. McRae, and J. E. Rowe, Phys. Rev. B **28**, 3656 (1983).

[24] K. Takayanaghi, Y. Tanishiro, M. Takahashi, and S. Takahashi, J. Vac. Sci. Technol. A **3**, 1502 (1985).

[25] E. J. van Loenen, A. E. M. J. Fischer, J. F. van der Veen, and F. LeGoues, Surf. Sci. **154**, 52 (1985).

[26] A. E. M. J. Fischer, P. M. J. Maree, and J. F. van der Veen, Appl. Surf. Sci. **27**, 143 (1986).

[27] R. Bruinsma and A. Zangwill, J. Phys. (Paris) **47**, 2055 (1986).

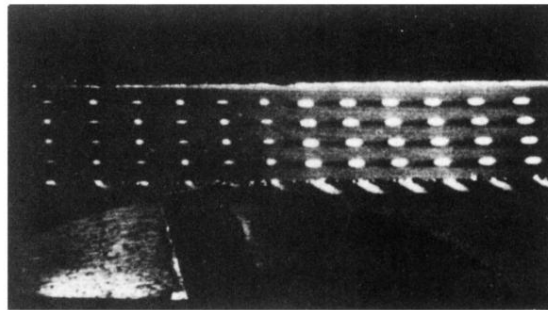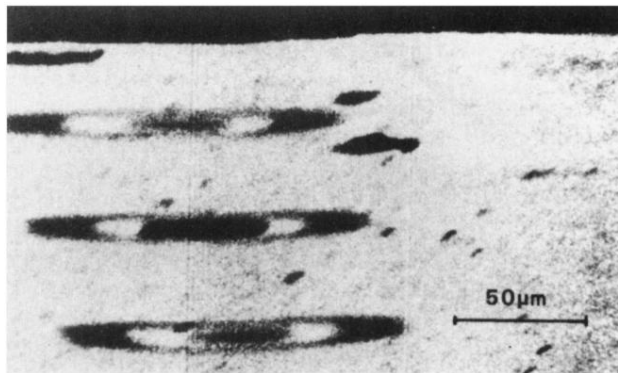[28] A. P. Johnson, M. S. thesis, Arizona State University, 1987 (unpublished).

FIG. 1. Dark field image of three annealed patches of nickel showing the NiSi$_2$ (B), NiSi$_2$ (A), and NiSi$_2$ ($A+B$) structures (top panel). Secondary electron image at low magnification (bottom panel).
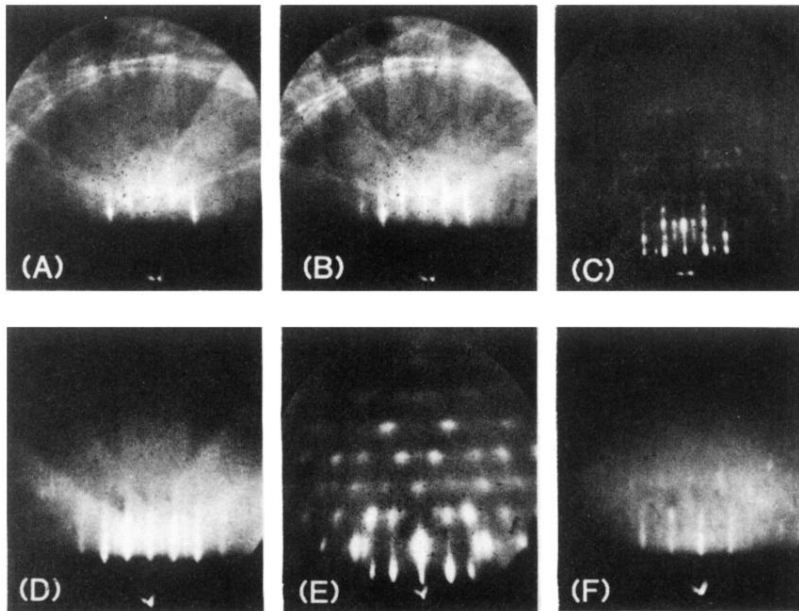
FIG. 2. RHEED patterns at 15 keV, [110] azimuth of (A) $NiSi_2$, (B) $NiSi_2$ (B), (C) Ni_2Si-δ (islands), (D) $NiSi_2$ ($A+B$), (E) Ni (islands), and (F) $\alpha+\beta$(NiSi).